applied sciences

MDPI

Article

Study on the Influence of Deep Soil Liquefaction on the Seismic Response of Subway Stations

Ming Shi, Lianjin Tao * and Zhigang Wang

Key Laboratory of Urban Security and Disaster Engineering, Ministry of Education, Beijing University of Technology, Beijing 100124, China; mings@emails.bjut.edu.cn (M.S.); zgwang@emails.bjut.edu.cn (Z.W.)
* Correspondence: ljtao@bjut.edu.cn

Abstract: Subway systems are a crucial component of urban public transportation, especially in terms of safety during seismic events. Soil liquefaction triggered by earthquakes is one of the key factors that can lead to underground structural damage. This study investigates the impact of deep soil liquefaction on the response of subway station structures during seismic activity, aiming to provide evidence and suggestions for earthquake-resistant measures in underground constructions. The advanced finite element software PLAXIS was utilized for dynamic numerical simulations. Non-linear dynamic analysis methods were employed to construct models of subway stations and the surrounding soil layers, including soil–structure interactions. The UBC3D-PLM liquefaction constitutive model was applied to describe the liquefaction behavior of soil layers, while the HS constitutive model was used to depict the dynamic characteristics of non-liquefied soil layers. The study examined the influence of deep soil liquefaction on the dynamic response of subway station structures under different seismic waves. The findings indicate that deep soil liquefaction significantly increases the vertical displacement and acceleration responses of subway stations compared to non-liquefied conditions. The liquefaction behavior of deep soil layers leads to increased horizontal effective stress on both sides of the structure, thereby increasing the horizontal deformation of the structure and posing a potential threat to the safety and functionality of subway stations. This research employed detailed numerical simulation methods, incorporating the non-linear characteristics of deep soil layer liquefaction, providing an analytical framework based on regulatory standards for evaluating the impact of deep soil liquefaction on the seismic responses of subway stations. Compared to traditional studies, this paper significantly enhances simulation precision and practical applicability. Results from this research indicate that deep soil layer liquefaction poses a non-negligible risk to the structural safety of subway stations during earthquakes. Therefore, the issue of deep soil liquefaction should receive increased attention in engineering design and construction, with effective prevention and mitigation measures being implemented.

Keywords: numerical simulation; deep liquefiable soil layer; subway station; acceleration; effective horizontal stress

Citation: Shi, M.; Tao, L.; Wang, Z. Study on the Influence of Deep Soil Liquefaction on the Seismic Response of Subway Stations. *Appl. Sci.* **2024**, *14*, 2307. https://doi.org/10.3390/app14062307

Academic Editors: Stefano Invernizzi and Igal M. Shohet

Received: 11 January 2024
Revised: 20 February 2024
Accepted: 7 March 2024
Published: 9 March 2024

1. Introduction

Earthquakes, with their suddenness, complexity, and severity, have severe impacts on human production and living conditions. Particularly in places with insufficient anti-seismic abilities and dense populations, the consequences caused by earthquakes are often extremely serious. Simultaneously, liquefaction behaviors triggered by earthquakes often lead to building collapse, underground facility damage, and other adverse results. Currently, the metro has become an important component of urban transportation. As areas where travelers gather and disperse, the seismic performance of metro stations, especially those located at liquefaction sites, is of particular importance.

In recent years, scholars have carried out importance research focusing on the seismic responses and damage mechanisms of subway stations in liquefied layers, obtaining

abundant research results. Wang, Jianning, Zhuang, and Haiyang et al. [1–3] analyzed the seismic response law of a hetero-span subway station in a liquefied field through the use of shaking table tests and numerical simulations; Tang Bozan, and Chen Su et al. [4,5] utilized a correlation analysis of the seismic responses of a subway station with irregular cross-sections in a liquefied site by means of shaking table tests; Chen Xiangsheng et al. [6] proposed and designed a replacement method for non-liquefied clay based on the concept of a "resilient city", and, through numerical simulation analysis, proved that this method has a good effect on resisting the liquefaction of the soil and reducing the uplift of the station structure; Liu Chunxiao et al. [7,8] conducted a detailed study on the seismic performance of monolayer two-span subway interval structures under different liquefaction location conditions through shaking table tests, and found that the liquefaction of soil at the bottom of the structure is the main cause of structural movement and inclined uplift; Zhang ZiHong and Xu ChengShun et al. [9,10] investigated the effect of liquefied interbedded soil on the seismic response of underground structures via centrifuge tests; Duan Yagang [11] conducted a shaker test to investigate the seismic response of subway stations in liquefied soil layers; Xu Minze et al. [12] analyzed the seismic response of burial depth on subway stations in liquefied sites; An Junhai et al. [13–17] studied the seismic performance of shield-expanded subway stations and frame subway stations in liquefied sites by means of shaking table tests and numerical simulations, investigating the damage mechanism of shield-expanded subway stations and the deformation mechanism of frame subway stations; Shun Liu et al. [18] conducted a numerical simulation to analyze the seismic response of a subway station embedded in saturated sand soil, revealing that the primary cause for the uplift of the station structure is the flow of liquefied sand soil beneath the station's base slab.

Based on the analysis above, it can be seen that studies have been conducted by scholars regarding the seismic response and failure mechanisms of metro stations with different structural forms in liquefied sites, including unconnected stations, standard stations, shield-driven stations, and sectional structures. Meanwhile, research has also been performed focusing on the impact of liquefied layers on underground structures. Studies show that the liquefaction behavior of ground soils affects the horizontal deformation, vertical displacement, and acceleration responses of station structures. The main research methods include numerical simulations, shaking table tests, and centrifuge tests. Among them, numerical simulations are beneficial due to characteristics such as visualization, cost-effectiveness, and wide applicability. Before a project's construction, this method can help engineers predict the seismic performance of metro station structures, including displacements, accelerations, and stresses, which are crucial for the seismic design of metro stations.

The Code for Seismic Design of Buildings [19] stipulates that if liquefied soil layers within a 20 m sub-surface range are identified, corresponding judgment criteria and mitigation measures will be provided based on the liquefaction level of the soil. However, no recommendations are offered for liquefied soil layers situated beyond a depth of 20 m. This lack of guidance leaves designers uncertain about how to address liquefied soil layers exceeding this depth. In practical engineering within the Beijing area, many subway stations have base plates buried more than 20 m deep, such as the Xidan and Wangfujing stations on Subway Line 1; the Xizhimen and Fuxingmen stations on Subway Line 2; and the Chongwenmen and Dongdan stations on Subway Line 5.

Should the embedding depth of a subway station's base slab reach 20 m, and should there be saturated sandy soil beneath, the possibility of liquefaction under seismic activity arises. The extent of such liquefaction and its impact on the subway station structure is not well-documented. *The Code for Seismic Design of Urban Rail Transit Structures* [20] indicates that, for station structures with base slabs embedded deeper than 20 m, it is necessary to conduct dedicated research on the liquefaction of deep soil layers (soil layers deeper than 20 m). Currently, research has been conducted by scholars regarding the consideration of liquefied soil layers below 20 m in depth. Abdulmuttalip Ari et al. [21] investigated

the impact of the depth of liquefied soil layers on the seismic response of piles through numerical simulation methods. The effect of structure–soil–structure interactions on seismic responses was studied by Konstantinos Kassas [22] using the finite difference software FLAC 5.0, which involved coupled hydrodynamic analysis. The issue of bearing capacity degradation caused by liquefaction in shallow foundations on two-layer soil profiles was explored through the use of numerical analysis by D.K. Karamitros [23]. By utilizing the characteristics of natural liquefied soil, Xenia Karatzia [24] isolated seismic protection structures and reduced the seismic impact on superstructures by partially repairing the surface soil, which then acted as a natural base isolation system. Araz Hasheminezhad [25] analyzed the seismic response of shallow foundations on liquefied soil which had been improved by deep soil mixing (DSM) via numerical simulations. The study examined the influence of the diameter and depth of DSM columns and the spacing and diameter of DSM column groups on the bearing capacity and settlement of shallow foundations, thus offering new insights for practical engineering applications.

The study aimed to investigate the seismic performance of subway stations under specific geological conditions, particularly when soil layers with potential liquefaction hazards exist beneath the station slabs. The significance of this issue lies in the safe operation of the subway system and the reliability of urban infrastructures. In light of this, the research focused on the specific case of a subway project in the Beijing area, where the complex geological environment and high population density both make safety requirements for subterranean structures exceedingly stringent.

In the process of conducting research, a geological model of the study subject was initially established based on field surveys and geological exploration results. This model encompasses the physical and mechanical properties of the soil layers, as well as the distribution of liquefiable strata. Given the approximate 20 m depth of the subway station's base slab, potential issues arising from soil liquefaction include an increase in buoyancy and variations in lateral earth pressure, all of which could impact the structural safety and functionality of the underground structure.

The method of numerical simulation was selected for seismic response analysis, permitting the performance evaluation of the structure under various hypothetical conditions without disrupting actual engineering operations. In order to ensure the accuracy and practicality of the study, relevant codes [20], were referred to, thus ensuring the scientific and rational nature of the analysis methods and results. Ultimately, it is anticipated that the outcomes of this study will provide robust technical support and suggestions for the design and construction of subway stations under similar geological conditions.

2. The Numerical Modeling

This article focuses on the seismic response of subway stations when the embedment depth of the station's base slab reaches 20 m, and yet a liquefiable soil layer still exists beneath the base slab. The main research approach is as follows:

(1) The soil layer above the station's base slab is simplified as a non-liquefiable layer, while the layer beneath is simplified as a liquefiable layer.

(2) The HS constitutive model is adopted for the non-liquefiable soil layer, the UBC3D-PLM constitutive model for the liquefiable layer, and an elastic constitutive model for the station structure; material parameters are selected based on the site investigation data.

(3) Two conditions, liquefied and non-liquefied, are established. The impact of the liquefiable soil layer on the subway station's seismic response is analyzed by inputting the design earthquake (E2 action) and the high-level earthquake (E3 action).

2.1. Computational Background

The context for this study is a subway station project in the Beijing area of China that involves a three-story, three-span standard station (shown in Figure 1). The top slab of the station has a cover soil thickness of 2.4 m, and its bottom slab is buried at a depth of 20 m.

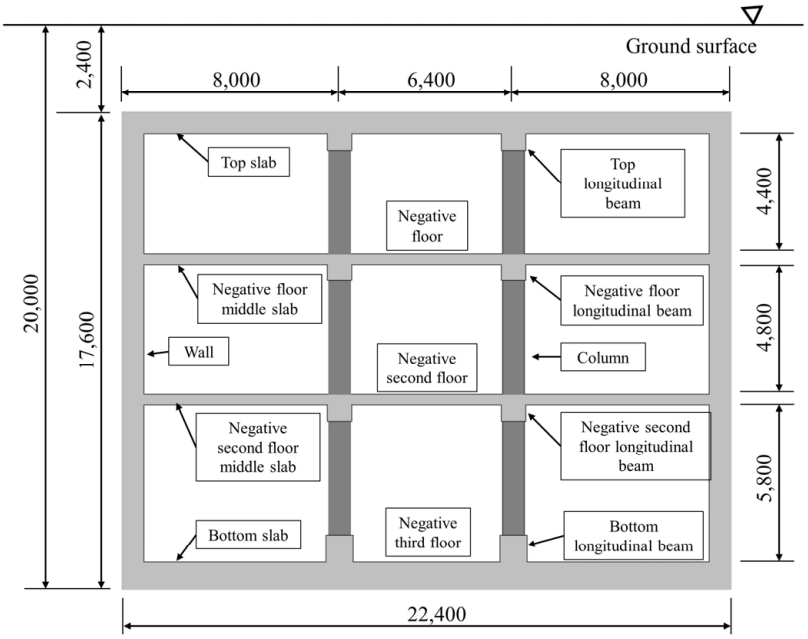

Figure 1. Cross-section of the subway station/mm.

The dimensions of its parts and concrete strength classes are shown in Table 1.

Table 1. Dimensions and concrete strength classes of various parts of the subway station.

Parts	Dimension/mm	Concrete Strength/MPa
Top slab	800	40
Negative floor middle slab	400	40
Negative second floor middle slab	400	40
Bottom slab	1000	40
Wall	800	40
Top longitudinal beam	900 × 1400	40
Negative floor longitudinal beam	900 × 1000	40
Negative second floor longitudinal beam	900 × 1000	40
Bottom longitudinal beam	1000 × 2000	40
Column	800 × 1200	40

2.2. Computational Modeling and Meshing

A constitutive model named UBC3D-PLM [26] was used by PLAXIS (www.bentley.com/en/products/brands/plaxis accessed on 1 March 2024) to describe the liquefaction behavior of soils, which is able to accurately characterize the change in the mechanical properties and liquefaction behavior of saturated sandy soils under cyclic loading. The model mainly consists of the bulk modulus K and shear modulus G to describe the nonlinear elastic behavior of the soil (see Equations (1) and (2)).

$$K = K_{\mathrm{B}}^{e} P_{\mathrm{A}} \left(\frac{p}{p_{ref}} \right)^{me} \tag{1}$$

$$G = K_{\mathrm{G}}^{e} P_{\mathrm{A}} \left(\frac{p}{p_{ref}} \right)^{ne} \tag{2}$$

K_{B}^{e} and K_{G}^{e} are the bulk modulus and shear modulus at the reference stress, respectively. The parameters ne and me determine the stress dependence. The reference stress p_{ref} is usually considered to be the atmospheric pressure (100 kPa).

The model initially employs the Mohr–Coulomb yield criterion for the primary loading phase, and utilizes a yield surface with a kinematic hardening rule for secondary loading. Upon the stress state reaching the yield surface, an immediate reversion to the elastic regime is not observed, thus enabling the prediction of plastic behavior. More specifically, strain hardening principles based on plasticity hardening are incorporated into the model. The structure of the station adopted in this article is characterized by a continuous, regular longitudinal form with an invariant transverse section, allowing for an approximate treatment as a plane strain problem, in accordance with the provisions of *The Code for Seismic Design of Urban Rail Transit Structures*. A two-dimensional computational model with dimensions of 340 m in width and 70 m in height has been established, encompassing soil layers, structures, and contact surfaces. The mesh size division should be less than one-eighth to one-tenth of the wavelength, corresponding to the highest frequency of the seismic waves. This is to prevent the mesh size from influencing the spectral characteristics of the seismic waves. The division of the model grid is illustrated in Figure 2.

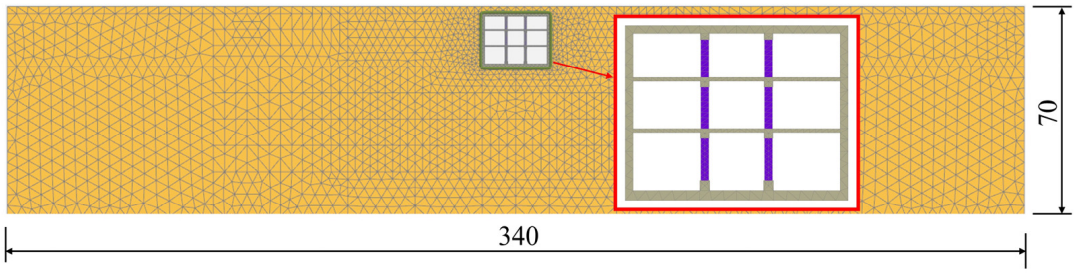

Figure 2. Mesh division/m.

2.3. Material Parameters

The constitutive model of the liquefied soil was taken from the UBC3D-PLM model, and the parameters are shown in Table 2. The Hensel–Spittel model was used for the constitutive model of the non-liquefied soil, and the parameters are shown in Table 3. The station structure was modeled using a linear elastic constitutive model with specific parameters, as shown in Table 4.

Table 2. Liquefied soil parameters.

Parameter	Symbol	Value	Unit
Constitutive model	/	UBC3D-PLM	/
Drain type	/	Undrain-A	/
Natural unit weight	γ_{unsat}	17	kN/m^3
Saturated unit weight	γ_{sat}	20	kN/m^3
Elastic Bulk Modulus factor	k_B^{*e}	749	/
Elastic Shear Modulus factor	k_G^{*e}	1069	/
Plastic shear modulus factor	k_G^{*p}	822	/
Elastic bulk modulus index	m_e	0.5	/
Elastic shear modulus index	n_e	0.5	/
Plastic shear modulus index	n_p	0.4	/
Friction angle	φ	35	°
Cohesion	c	0	kPa
SPT value	$(N_1)_{60}$	15	time
Magnification factor	f_{dens}	1	/
Post-liquefaction factor	f_{Epost}	1	/
Atmospheric pressure	P_{ref}	100	kPa
Failure ratio	R_f	0.7328	/

Table 3. Parameters of non-liquefied soil.

Parameter	Symbol	Value	Unit
Constitutive model	/	Hensel-Spittel	/
Drains type	/	Drain	/
Natural unit weight	γ_{unsat}	17	kN/m^3
Saturated unit weight	γ_{sat}	20	kN/m^3
Deformation modulus	E_{50}^{ref}	1.8×10^4	kPa
Compression modulus	E_{oed}^{ref}	1.8×10^4	kPa
Unloaded Modulus	E_{ur}^{ref}	5.4×10^4	kPa
Power index	m	0.5	/
Cohesion	c	0	kPa
Friction angle	φ	35	°
Trimmed angle	ψ	0	°

Table 4. Station structural parameters.

Parameters	Symbol	Value	Unit
Constitutive model	/	Linear elasticity	/
Drains type	/	Dry	/
Unit weight	γ	25	kN/m^3
Elastic modulus	E	3.25×10^7	kPa
Poisson's ratio	ν	0.2	/

2.4. Seismic Wave Selection

In this paper, the seismic record (called Beijing Hotel wave) obtained from the Beijing Hotel station during the 1976 Tangshan earthquake is selected, with a peak acceleration of 0.385 g and a duration of 50 s. The time history and Fourier spectrum of the seismic wave are both shown in Figure 3.

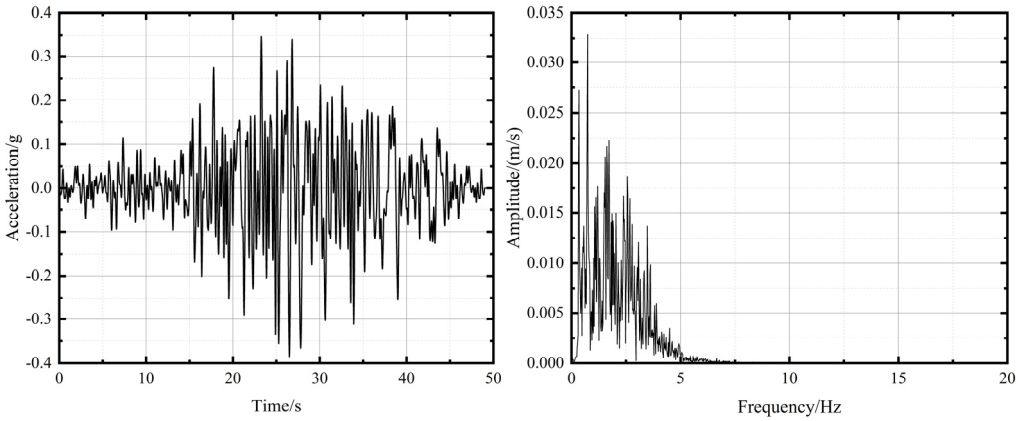

Figure 3. Beijing Hotel Tangshan earthquake wave time history curve and Fourier spectrum.

2.5. Loading Case Setting

The seismic waves are the input from the bottom of the model, and the peak ground acceleration values are determined to be 0.2 g and 0.4 g via free-field calculations; these values correspond to the design earthquake and high-level earthquake in *The Code for seismic design of urban rail transit structures* (GB50909-2014). The specific case settings are shown in Table 5.

Table 5. Case setting.

Case	Earthquake	Symbol	PGA/g	Liquefaction Situation
1	Design earthquake	E2	0.2	Non-liquefaction
2	Design earthquake	E2	0.2	Deep liquefaction
3	High-level earthquake	E3	0.4	Non-liquefaction
4	High-level earthquake	E3	0.4	Deep liquefaction

Before the dynamic calculations, the soil, structure, and contact surfaces for the static calculations were activated. Next, the effective stress and static pore water pressure of the soil layer under static conditions were obtained. Then, the soil constitutive model considering the liquefaction behavior was replaced with the UBC3D-PLM model. The static boundary conditions were then replaced with free-field boundary conditions. After this, the dynamic loads were activated. The dynamic loading situation is shown in Figure 4.

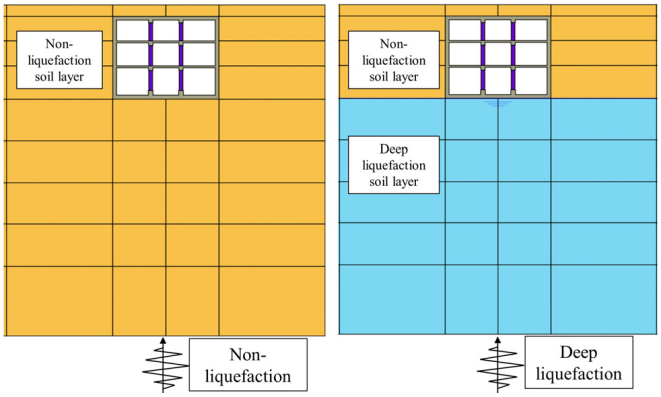

Figure 4. Loading situations.

3. Calculation Results Analysis of Soil Layers

Monitoring points have been established for the extraction of seismic response data from soil layers. The selection of monitoring points is illustrated in Figure 5. Within this figure, the symbol A represents the acceleration measurement points, symbol P denotes the pore pressure ratio measurement points, and symbol T signifies horizontal effective stress measurement points.

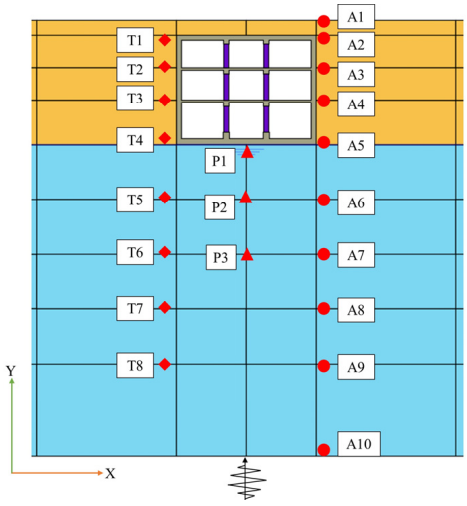

Figure 5. Arrangement of monitoring points in the soil.

3.1. Acceleration of Soil Layers

The distribution of the peak acceleration along the vertical direction in the soil layer is shown in Figure 6. The peak acceleration in the soil layer tends to be amplified from the bottom of the model to the model surface. When subjected to the conditions of the design earthquake (E2), the peak acceleration of the soil layer located below A7 shows that Case 1 is greater than Case 2, and the peak acceleration of the soil layer located above A7 shows that Case 1 is less than Case 2. Under the action of the high-level earthquake (E3), the peak acceleration of the soil layer located below A6 shows that Case 3 is larger than Case 4, and the peak acceleration of the soil layer located above A6 shows that Case 3 is smaller than Case 4. This indicates that the deep liquefied soil layer has a significantly greater effect on the acceleration response of the soil layer near the structure than the non-liquefied soil layer.

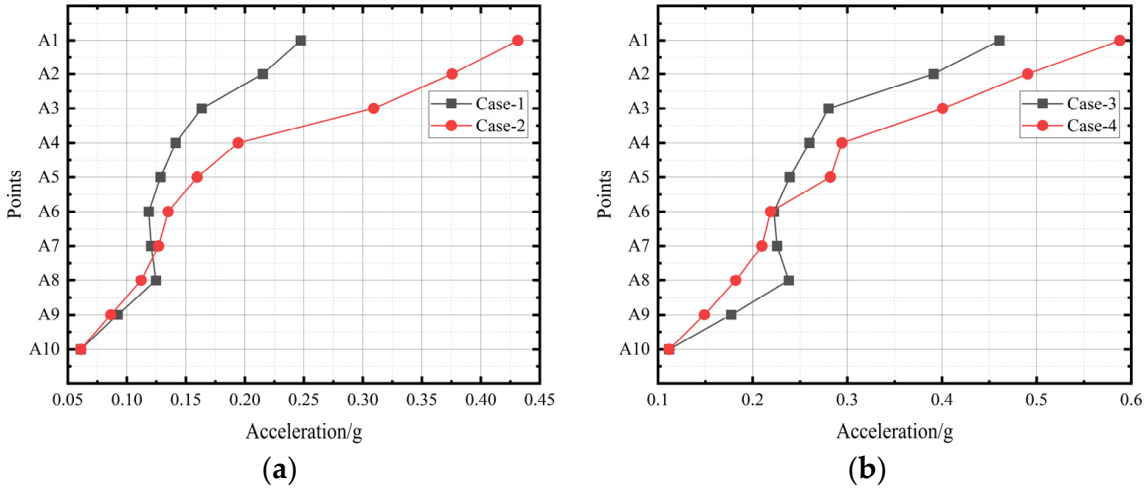

Figure 6. Vertical distribution of peak acceleration of soil. (**a**) design earthquake; (**b**) high-level earthquake.

3.2. Pore Pressure Ratio

The liquefaction characteristics of the soil layer beneath the station structure's bottom slab have been investigated. The pore pressure ratio (ppr) is employed to depict the liquefaction behavior of the soil. The soil layer is fully liquefied when the ppr = 1. As demonstrated in Figure 7, the liquefied region is principally located below the structure's bottom slab under the impact of the design earthquake. Under the influence of the high-level earthquake, the liquefied areas primarily extend directly below the structure and, to a certain extent, on both sides of the bottom slab.

The pore pressure ratio curve is shown in Figure 8. P1 is located at the bottom slab of the station, P2 is located 10 m under the bottom slab of the station, and P3 is located 20 m under the bottom slab of the station. The magnitude of the pore pressure ratio under the effect of the design earthquake is P1 > P2 > P3, where the peak pore pressure ratio of P1 is close to 0.5. The magnitude of the pore pressure ratio under the effect of the high-level earthquake is P1 > P2 > P3, where the peak pore pressure ratio of P1 reaches 0.8. This indicates that the soil experiences a high degree of liquefaction at the bottom slab of the station structure under the action of the high-level earthquake. The degree of liquefaction in the deep liquefied soil layers is directly proportional to the seismic intensity. Under the action of the high-level earthquake, the soil layer at the bottom slab of the station structure is close to complete liquefaction.

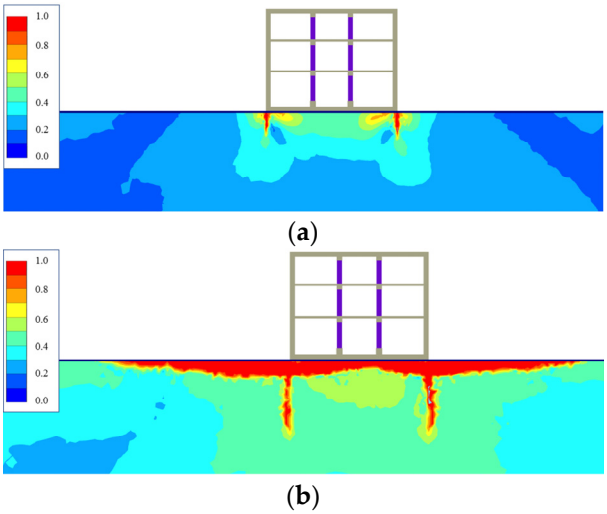

Figure 7. Cloud diagram of the pore pressure ratio: (**a**) design earthquake; (**b**) high-level earthquake.

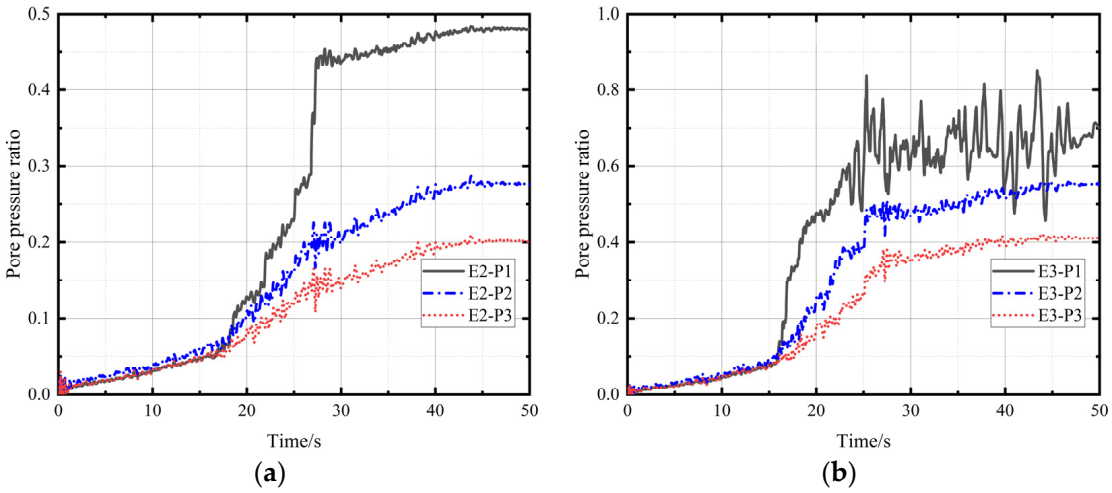

Figure 8. Pore pressure ratio curves for different seismic intensities: (**a**) design earthquake; (**b**) high-level earthquake.

3.3. Horizontal Effective Stresses in Soil Layers

The effective stresses in the x-direction at each point for the design earthquake and the high-level earthquake are shown in Tables 6 and 7, respectively. Regardless of whether it is the design earthquake or the high-level earthquake, the peak effective stresses at points T1 to T4 in the case of non-liquefaction are smaller than those in the case of deep liquefaction; in addition, the peak effective stresses at point T5 to T8 in the case of non-liquefaction are larger than those in the case of deep liquefaction. This suggests that the deep liquefied soil layer will only weaken its own effective stresses in the x-direction, whereas it will have a strong amplifying effect on the effective stresses in the soil layers which are located on both sides of the structure. When compared to the non-liquefaction case, the increase in the effective stresses in the soil layers on both sides of the station structure in the deep liquefaction case under the action of the design earthquake ranged from 4.9% to 24.7%. The increase in the effective stresses in the soil layers on both sides of the station structure in the deep liquefaction case under the action of a high-level earthquake ranged from 22.1% to 48.8%. It is shown that the effect of the deep liquefied soil layer on the effective stresses in the soil layers on both sides of the structure increases with the seismic intensity.

Table 6. Effective stresses in the x-direction of the soil layer under the design earthquake (kPa).

Points	Case 1	Case 2	Case 2 − Case 1	Amplitude/%
T1	41.82	43.99	2.17	4.9
T2	67.18	89.18	22.00	24.7
T3	100.85	132.88	32.03	24.1
T4	153.98	186.63	32.65	17.5
T5	221.40	220.95	−0.45	−0.2
T6	285.80	279.98	−5.82	−2.0
T7	348.97	320.13	−28.84	−8.3
T8	410.39	349.67	−60.72	−14.8

Table 7. Effective stresses in the x-direction of the soil layer under the high-level earthquake (kPa).

Points	Case 3	Case 4	Case 4 − Case 3	Amplitude/%
T1	49.71	71.69	21.98	30.7
T2	95.42	122.55	27.13	22.1
T3	127.16	184.61	57.45	31.1
T4	185.45	362.31	176.86	48.8
T5	260.93	223.94	−36.99	−14.2
T6	329.38	294.93	−34.45	−10.5
T7	393.29	349.94	−43.35	−11.0
T8	450.56	395.65	−54.91	−12.2

4. Analysis of the Calculation Results of the Station Structure

The arrangement of the points used to monitor the top slab of the station structure and its center column is shown in Figure 9.

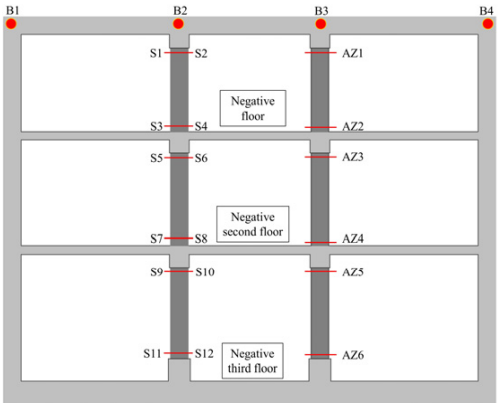

Figure 9. Arrangement of station structure measurement points.

4.1. Vertical Displacement of the Structure

The vertical displacement of the station structure is shown in Figure 10. Under the action of the design earthquake, the amount of structural uplift in the deep liquefaction case is greater than that in the non-liquefaction case, but the difference between the two is not significant. The difference between the amount of structural uplift in the deep liquefaction case and that found in the non-liquefaction case is large under the high-level earthquake. This indicates that the liquefaction behavior of the deep liquefied soil layer has an effect on the uplift of the structure, and the higher the degree of liquefaction, the more obvious the observed uplift trend in the structure.

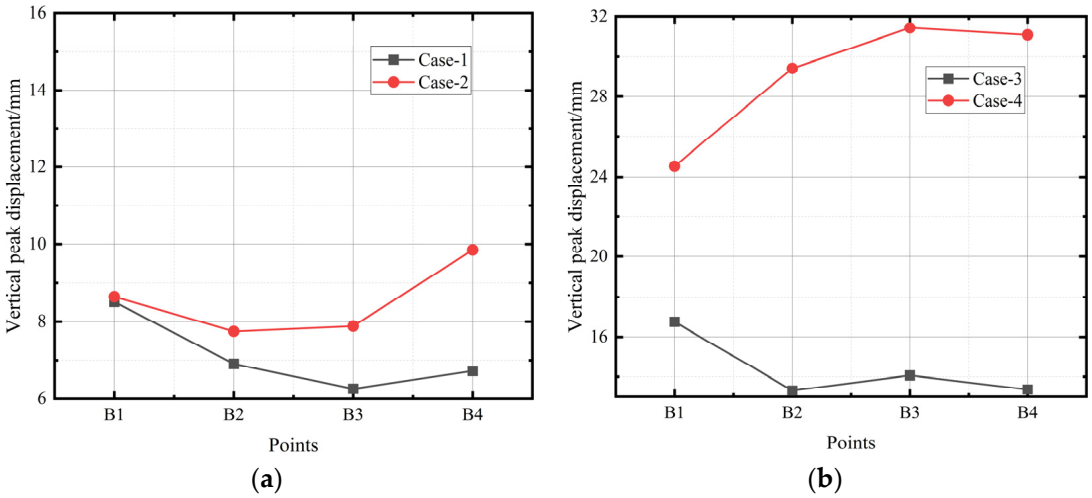

Figure 10. Vertical displacement of the top slab of the station structure: (**a**) design earthquake; (**b**) high-level earthquake.

4.2. Structural Interlayer Displacements

The results of the calculation of the interlayer displacement angle of the station structure are shown in Table 8. The interlayer displacement angle for Case 2 was greater than that for Case 1, and the interlayer displacement angle for Case 4 was slightly greater than that for Case 3. Under the action of the design earthquake, the horizontal deformation performance of the structure in the case of a deep liquefied soil layer is greater than that in the case of a non-liquefied soil layer. The horizontal deformation performance of the structure in the case of deep liquefied soil layers is close to that observed in the case of non-liquefied soil layers under the action of a high-level earthquake.

Table 8. Interlayer displacement angles of station structures.

Position	Design Earthquake		High-Level Earthquake	
	Case 1	Case 2	Case 3	Case 4
Negative floor	1/725	1/446	1/386	1/371
Negative second floor	1/444	1/264	1/242	1/232
Negative third floor	1/506	1/309	1/298	1/283

4.3. Acceleration Response of Center Column

The results of the peak acceleration calculations for the columns in the station structure are shown in Table 9. The peak acceleration of the column in the structure for Case 1 is less than that for Case 2 under the action of the design earthquake. The peak acceleration of the structural center column for Case 3 is less than that for Case 4 under the effect of the high-level earthquake. It is shown that the deep liquefied soil layer causes an increase in the acceleration response of the columns in the station structure, regardless of the seismic intensity.

Table 9. Peak acceleration of columns in the station structure (g).

Points	Design Earthquake/g		High-Level Earthquake/g	
	Case 1	Case 2	Case 3	Case 4
AZ1	0.21	0.37	0.39	0.50
AZ2	0.17	0.30	0.29	0.41
AZ3	0.16	0.29	0.27	0.38
AZ4	0.14	0.20	0.25	0.29
AZ5	0.14	0.18	0.25	0.29
AZ6	0.13	0.15	0.23	0.28

4.4. Peak Tensile Stresses in Center Columns

The peak tensile stresses calculated for the columns in the station structure are shown in Table 10. The peak tensile stress in the center column for Case 1 is less than that for Case 2. The peak tensile stress in the center column for Case 3 is less than that for Case 4. The liquefaction behavior of the deep liquefied soil layers always increases the tensile stress response of the columns in the station structure, regardless of the seismic intensity.

Table 10. Peak tensile stress in center column (kPa).

Points	Design Earthquake/kPa		High-Level Earthquake/kPa	
	Case 1	Case 2	Case 3	Case 4
S1	582	2831	2231	4196
S2	3291	4164	5479	4547
S3	1816	2339	3182	2597
S4	81	1460	1116	2346
S5	783	2476	1964	3267
S6	1554	2272	3154	2520
S7	1485	2184	3094	2597
S8	581	2195	1758	3202
S9	474	2272	1954	2329
S10	2538	3275	3367	4651
S11	4238	5396	5537	7467
S12	1389	4129	3633	4241

5. Discussion

The primary objective of this study is to assess how the liquefaction behavior of a deep liquefiable soil layer, situated 20 m beneath the surface under the base slab of a subway station, influences the dynamic response of the station during seismic events. Detailed numerical simulations revealed significant liquefaction occurrences within this deep soil layer. These findings are in agreement with those reported by Yao Jiantao et al. [27], who also noted similar phenomena in their research on the impact of liquefiable soil layer positioning on the seismic responses of underground structures. The construction of subway stations has been shown to reduce the vertical effective stress on the soil layers below, thereby increasing the likelihood of soil liquefaction.

This article posits that the impact of the liquefaction depth should be taken into account in the design of subway stations, aligning with the recommendations made by Abdulmuttalip Ari et al. [21]. The liquefaction behavior of soil layers can lead to an increase in the pore water pressure and a reduction in effective stress within the soil, thus subsequently decreasing the bearing capacity of the soil beneath the station. These findings are in agreement with the research carried out by D.K. Karamitros [23] and Araz Hasheminezhad [25]. Under the conditions of deep soil layer liquefaction, the horizontal effective stress in the soil adjacent to subway stations increases by 20% to 50%, whereas the horizontal effective stress beneath the stations decreases by 2% to 15%. This phenomenon may be attributable to the reduction in soil effective stress caused by liquefaction, while the presence of structures tends to increase the effective stress within the soil. These results are consistent with the phenomena observed in the vibration table experiments concerning the impact of liquefied soil layer distribution on the seismic responses of underground structures conducted by Chunxiao Liu et al. [28].

It should be noted, however, that the distribution of soil layers was simplified in this study. In actual engineering practice, the characteristics of soil layer distribution can be determined based on geological exploration results. Hence, the applicability of the conclusions should be viewed only from a qualitative perspective.

Additionally, although frictional contact issues between soil layers and structures have been contemplated in this study, the characterization of normal and tangential frictional properties has been simplified. Future research could be enhanced by employing more advanced modeling techniques, such as the finite element method combined with multiscale

analysis. This would assist in a more precise assessment of the impact of liquefied soil on the dynamic response of subway station structures, providing more detailed references for seismic designs.

Overall, despite this study's revelation regarding the impact that the liquefaction behavior of deep soil layers has on the seismic response of subway stations, further experimental research is required for the validation and refining of the predictive capabilities of numerical models. Moreover, given the critical role of subway stations in urban transportation, it is recommended that future engineering practices incorporate an enhanced assessment of seismic risks for subway stations situated above liquefiable soil layers.

6. Conclusions

This study employs numerical simulations to investigate the seismic responses of subway stations situated in deep liquefiable soil layers. Comparative analysis with subway stations embedded in non-liquefiable soil strata has yielded the following principal conclusions:

(1) The liquefaction of deep soil layers significantly influences the seismic response of the strata; an appreciable increase in acceleration and horizontal effective stress is observed in the soil layers on both sides of the station structure; beneath the station structure, a marked decrease in acceleration and horizontal effective stress is noted.

(2) Although the liquefiable soil layer is located 20 m beneath the surface, seismic activity can still induce severe liquefaction of the soil beneath the base slab of the station structure, thus leading to the uplift of the station structure. This phenomenon suggests that the presence of the station structure reduces the vertical effective stress on the underlying soil, thereby increasing the likelihood of soil liquefaction.

(3) The influence of deep soil layer liquefaction on the seismic response of station structures is more pronounced. It is primarily manifested in indicators such as interstory displacement, the acceleration responses of central columns, and tensile stress in central columns.

This study also found that the uncertainty of soil layer parameters has a significant impact on the simulation results, which highlights the importance of field investigations.

Based on the conclusions drawn, it is recommended that both the design and construction of subway stations should integrate a comprehensive consideration of liquefaction risks and implement appropriate protective measures. Furthermore, to enhance the precision of seismic designs, future research should incorporate an expanded dataset from on-site testing and advanced simulation techniques to better simulate the impact of liquefaction on subway stations.

Author Contributions: Methodology, M.S. and L.T.; Validation, M.S. and L.T.; Data curation, M.S.; Writing—original draft, M.S.; Writing—review and editing, M.S. and Z.W.; Project administration, L.T. All authors have read and agreed to the published version of the manuscript.

Funding: This research was funded by [National Natural Science Foundation of China], grant number [42072308].

Institutional Review Board Statement: Not applicable.

Informed Consent Statement: Not applicable.

Data Availability Statement: Data are contained within the present article.

Conflicts of Interest: The authors declare no conflicts of interest.

References

1. Wang, J.; Fu, J.; Zhuang, H.; Dou, Y.; Ma, G. Seismic response analysis of complex subway station structure with unequal-span in liquefiable foundation. *J. Vib. Shock* **2020**, *39*, 170–179. (In Chinese)
2. Wang, J.; Yang, J.; Zhuang, H.; Fu, J.; Dou, Y. Shaking table test on liquefaction characteristics of foundation around a complicated subway station with diaphragm walls. *Chin. J. Geotech. Eng.* **2020**, *42*, 1858–1866. (In Chinese)

3. Wang, J.; Ma, G.; Zhuang, H.; Dou, Y.; Fu, J. Influence of diaphragm wall on seismic responses of large unequal-span subway station in liquefiable soils. *Tunn. Undergr. Space Technol. Inc. Trenchless Technol. Res.* **2019**, *91*, 102988. [CrossRef]
4. Tang, B.; Li, X.; Chen, S. Seismic deformation characteristics of liquefaction soil-irregular section underground structure. *J. Vib. Shock* **2020**, *39*, 217–225. (In Chinese)
5. Chen, S.; Tang, B.; Zhuang, H.; Wang, J.; Li, X.; Zhao, K. Experimental investigation of the seismic response of shallow-buried subway station in liquefied soil. *Soil Dyn. Earthq. Eng.* **2020**, *136*, 106153.
6. Yu, Y.; Bao, X.; Chen, X.; Shen, J.; Wang, S.; Cui, H. Study of the effect of seismic performance measures on a metro station structure in liquefiable soil. *Tunn. Undergr. Space Technol. Inc. Trenchless Technol. Res.* **2023**, *131*, 104760. [CrossRef]
7. Liu, C.; Tao, L.; Bian, J.; Zhang, Y.; Feng, J.; Dai, X.; Wang, Z. Shaking table test of seismic effect of liquefiable soil layer on underground structure. *J. Zhejiang Univ.* **2021**, *55*, 1327–1338. (In Chinese)
8. Liu, C.; Tao, L.; Bian, J.; Zhang, Y.; Feng, J. Experimental Design of Shaking Table Test on Seismic Response of Soil and Underground Structures in Liquefiable Soil. *J. Disaster Prev. Mitig. Eng.* **2022**, *42*, 1341–1350. (In Chinese)
9. Zhang, Z.; Xu, C.; Yan, G.; Du, X.; Li, Y.; Zhou, Y. Experimental design for dynamic centrifuge tests on a subway station structure in liquefied interlayer site. *Chin. J. Geotech. Eng.* **2022**, *44*, 879–888. (In Chinese)
10. Yan, G.; Xu, C.; Zhang, Z. Influence of soil-structure interface characteristics on seismic response of underground structure in the local liquefaction interlayer site. *Chin. J. Rock Mech. Eng.* **2023**, *42*, 3643–3653. (In Chinese)
11. Duan, Y. Shaking Table Research on the Response of Subway Underground Structure under Earthquake Liquefaction. *J. Railw. Eng. Soc.* **2019**, *36*, 75–79. (In Chinese)
12. Xu, M.; Cui, C.; Yao, Y.; Wang, G.; Liang, Z.; Li, C.; Wang, Q. Influence of burial depth on the seismic response of subway station in liquefiable subgrade. *J. Shen Zhen Univ. Sci. Eng.* **2020**, *37*, 287–292. (In Chinese) [CrossRef]
13. An, J.; Tao, L.; Jiang, L. A shaking table-based experimental study on seismic response of a shield- enlarge-dig type subway station structure. *Rock Soil Mech.* **2022**, *43*, 1277–1288. (In Chinese)
14. An, J.; Tao, L.; Jiang, L.; Yan, H. A shaking table-based experimental study of seismic response of shield-enlarge-dig type's underground subway station in liquefiable ground. *Soil Dyn. Earthq. Eng.* **2021**, *147*, 106621. [CrossRef]
15. An, J. Study on Shaking Table Test of Underground Subway Structure in Liquefiable Site and Seismic Design Method. Ph.D. Thesis, Beijing University of Technology, Beijing, China, 2017. (In Chinese)
16. An, J.; Yan, H.; Zhao, Z.; Jiang, L. Seismic Response Analysis of Liquefiable Soil Layer on Subway Station Structure. *Sci. Technol. Eng.* **2022**, *22*, 7080–7088. (In Chinese)
17. An, J.; Liu, Q.; Zhang, Y.; Zhang, X. Seismic Response Comparisons of Prefabricated and Cast In Situ Subway Station Structures in Liquefiable Site. *Buildings* **2023**, *13*, 3071. [CrossRef]
18. Liu, S.; Tang, X.; Luan, Y.; Ahmad, M. Seismic response analysis of subway station in deep loose sand using the ALE method. *Comput. Geotech.* **2021**, *139*, 104394. [CrossRef]
19. *GB50011-2010*; Code of Seismic Design of Buildings. China Construction Industry Press: Beijing, China, 2010.
20. *GB50909-2014*; Code for Seismic Design of Urban Rail Transit Structures. China Planning Press: Beijing, China, 2014.
21. Ari, A.; Demir, S.; Özener, P. Examining the Role of Liquefiable Layer Thickness and Depth on the Seismic Lateral Response of Piles through Numerical Analyses. *Int. J. Geomech.* **2023**, *23*, 04023047. [CrossRef]
22. Kassas, K.; Adamidis, O.; Anastasopoulos, I. Structure–soil–structure interaction (SSSI) of adjacent buildings with shallow foundations on liquefiable soil. *Earthq. Eng. Struct. Dyn.* **2022**, *51*, 2315–2334. [CrossRef]
23. Karamitros, D.K.; Bouckovalas, G.D.; Chaloulos, Y.K.; Andrianopoulos, K.I. Numerical analysis of liquefaction-induced bearing capacity degradation of shallow foundations on a two-layered soil profile. *Soil Dyn. Earthq. Eng.* **2013**, *44*, 90–101. [CrossRef]
24. Karatzia, X.; Mylonakis, G.; Bouckovalas, G. Seismic isolation of surface foundations exploiting the properties of natural liquefiable soil. *Soil Dyn. Earthq. Eng.* **2019**, *121*, 233–251. [CrossRef]
25. Hasheminezhad, A.; Bahadori, H. Seismic response of shallow foundations over liquefiable soils improved by deep soil mixing columns. *Comput. Geotech.* **2019**, *110*, 251–273. [CrossRef]
26. Petalas, A.; Galavi, V. *Plaxis Liquefaction Model UBC3D-PLM.*; Delft University of Technology: Delft, The Netherlands, 2013.
27. Yao, J.; Lin, Y. Influence Analysis of Liquefiable Interlayer on Seismic Response of Underground Station Structure. *Appl. Sci.* **2023**, *13*, 9210. [CrossRef]
28. Liu, C. Shaking Table Test on Influence of Liquefiable Soil Distribution on Seismic Response of Soil and Subway Underground Structures. *China Railw. Sci.* **2021**, *42*, 30–40. (In Chinese)